Biophysical Chemistry 200–201 (2015) 1–8

Contents lists available at ScienceDirect

Biophysical Chemistry

journal homepage: http://www.elsevier.com/locate/biophyschem

Spectrin–ankyrin interaction mechanics: A key force balance factor in the red blood cell membrane skeleton

Masakazu Saito [a,*], Takahiro Watanabe-Nakayama [a], Shinichi Machida [a], Toshiya Osada [c], Rehana Afrin [a,b], Atsushi Ikai [a]

[a] Innovation Laboratory, Tokyo Institute of Technology, 4259 Nagatsuta-cho, Midori-ku, Yokohama, Kanagawa 226-8501, Japan
[b] Biofrontier Center, Tokyo Institute of Technology, 4259 Nagatsuta-cho, Midori-ku, Yokohama, Kanagawa 226-8501, Japan
[c] Depertment of Life Science, Graduate School of Bioscience and Biotechnology, Tokyo Institute of Technology, B-2 4259 Nagatsuta-cho, Midori-ku, Yokohama, Kanagawa 226-8501, Japan

HIGHLIGHTS

- Spectrin–ankyrin unbinding force was obtained at the single molecule level.
- A mean unbinding force centered around 30 pN.
- Two energy barriers in the unbinding process were identified.

GRAPHICAL ABSTRACT

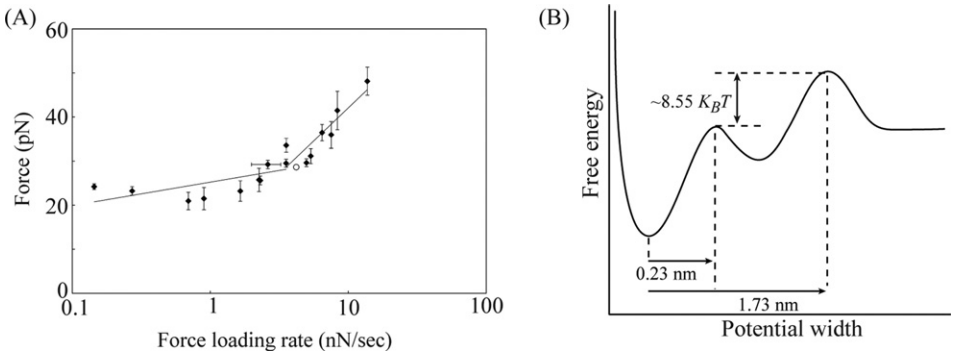

ARTICLE INFO

Article history:
Received 29 January 2015
Received in revised form 19 March 2015
Accepted 22 March 2015
Available online 28 March 2015

Keywords:
Dynamic force microscopy
Protein–protein interaction
Spectrin
Ankyrin
Membrane skeleton

ABSTRACT

As major components of red blood cell (RBC) cytoskeleton, spectrin and F-actin form a network that covers the entire cytoplasmic surface of the plasma membrane. The cross-linked two layered structure, called the membrane skeleton, keeps the structural integrity of RBC under drastically changing mechanical environment during circulation. We performed force spectroscopy experiments on the atomic force microscope (AFM) as a means to clarify the mechanical characteristics of spectrin–ankyrin interaction, a key factor in the force balance of the RBC cytoskeletal structure. An AFM tip was functionalized with ANK1-62k and used to probe spectrin crosslinked to mica surface. A force spectroscopy study gave a mean unbinding force of ~30 pN under our experimental conditions. Two energy barriers were identified in the unbinding process. The result was related to the well-known flexibility of spectrin tetramer and participation of ankyrin 1–spectrin interaction in the overall balance of membrane skeleton dynamics.

1. Introduction

A typical human red blood cell (RBC) makes hundreds of thousands of circulations through blood vessels and capillaries during its average life time of 120 days. Some of the capillaries have diameters less than

* Corresponding author at: Graduate School of Arts and Sciences, The University of Tokyo, 3-8-1, Komaba, Meguro-ku, Tokyo, 153-8902, Japan. Tel./fax: +81 3 5454 6628.
E-mail address: saito_m@bio.c.u-tokyo.ac.jp (M. Saito).

http://dx.doi.org/10.1016/j.bpc.2015.03.007
0301-4622/

that of RBC itself. It is, therefore, necessary for RBCs to change their shape rather drastically to flow alternately through narrow capillaries and wider blood vessels [1]. Furthermore, RBCs are also under various types of shear stress even in larger blood vessels especially where blood flow is turbulent. RBCs are therefore equipped with a well developed membrane system with mechanical flexibility and resilience to withstand drastic and repetitious shape changes [2,3].

As introduced above, the membrane system of RBC has a composite lamellar structure of lipid bilayer on the outer and a proteinaceous cytoskeleton on the cytoplasmic side [4]. The cytoskeleton is made of a 2D regular array of the filamentous protein, spectrin tetramers, with a six-fold connectivity to the structure called the hub which is composed of a short F-actin filament and several other proteins [5]. The spectrin–actin cytoskeleton forms a continuous 2D network lining the cytoplasmic side of the plasma membrane. The network has, in average, ~3.2×10^4 hubs and ~10^5 spectrin tetramers [6]. The network is periodically connected to the plasma membrane through linking proteins including ankyrin and Band 4.1. Ankyrin, on its one end, is non-covalently bound to cytoskeletal spectrin and, on the other, to Band 3 in the plasma membrane.

In its biconcave form, the RBC has a capacity to absorb mechanical stresses without significant increase in the overall energy and, therefore, capable of flexibly changing the entire cell shape according to environmental requirements [7,8]. This global flexibility of the cell comes mainly from a large surface area/volume ratio and from the physical nature of the membrane skeleton. The largely fluidic cytoplasmic resistance to shape changes is negligible. Such reversible flexibility is believed to originate from a combination of unique mechanical properties of phospholipid bilayer membrane and proteinaceous cytoskeleton (for example, [1]).

The basic spectrin dimer is composed of a pair of α- and β-spectrin subunits [9]. Both subunits form triple helical filamentous structures which associate themselves to form a high molecular weight heterodimer [10]. In human erythroid spectrin heterodimer shows the triplet helical repeats such as spectrin repeats. The 37 spectrin repeats are present in the spectrin heterodimer [10]. The repeats 14 and 15 of the β-spectrin repeats are recognized by ZU5 domain of ankyrin [10,11]. In its functional state, two hetero-dimers are assembled into a tetramer in a head-to-head fashion. The contour length of a self-assembled tetramer is about 200 nm but an estimated *in vivo* end-to-end distance is 70 nm in average, reflecting a relaxed condition of the molecule [8]. Spectrin tetramers span two actin hub sites in a conformationally relaxed state allowing a mild degree of compression and/or extension with only a small energy change [1,8]. Experimentally, the delipidated cytoskeleton of human RBC has recently been shown to be stretched up to a few micrometers under a very small tensile stress [12].

To understand the biological roles of cytoskeletal spectrin, we need to investigate its mechanical balance that enables an RBC to maintain a highly flexible and resilient geodesic network structure.

Some mechanical properties of the folded structure of spectrin have been elucidated by several groups by the force spectroscopy method on the atomic force microscope (AFM) [13,14]. Spectrin, in such experiments, was adsorbed on a mica substrate and then the protein was pulled by the cantilever tip of the AFM. The immobilized spectrin was gradually extended under an increasing tensile stress until it was completely unfolded, allowing the investigators to trace the force curve of the unfolding process. They observed a train of small force peaks corresponding to unfolding of tandemly repeating domain structures within a single spectrin molecule. A similar observation has been reported on the ankyrin unfolding process [15].

Ankyrin forms a protein family that links certain integral membrane proteins to the underlying cytoskeletal structures in various cell types [16]. Proteins of the ankyrin family play key roles in cellular activities such as cell motility, regulation by extensive differential mRNA splicing, contact and the maintenance of specialized membrane domains.

It has been demonstrated that erythrocyte ankyrin is linked to the integral membrane protein, Band 3, on one end and to the cytoskeletal spectrin on the other. As manifested by this example, the static as well as dynamical structure of erythrocyte membrane–cytoskeleton system is entirely maintained through non-covalent association of component proteins, namely, spectrin, actin, ankyrin, Band 3, Band 4.1, glycophorin C and a few others [17].

The resilient nature of RBC membrane skeleton attracted interest of wide ranging researchers. There have been a numerous studies on the mechanics and dynamics of the reversible shape change of RBC under artificially imposed stresses [18,19]. It is widely recognized that the most important factor of this remarkable nature of the membrane skeleton system is in the rubber-like flexibility of spectrin tetramers [1] with or without unfolding of its tertiary structure [20,21]. An additional mechanism proposed for dissipation of the stress energy is cyclically repeating dissociation and re-association of its component protein pairs [22]. Whether any of these proposed mechanisms is actually involved in the cyclic deformation and recovery of RBC conformation, and, if so, to what extent is not easy to be assessed. We believe that determination of the unbinding force of each pair of non-covalently associated proteins would at least give a most straightforward clue to answer such questions. We will then be able to understand the mechanical balance of the membrane skeleton network system.

As a part of our continued interest in the mechanical setup of cytoskeleton, we decided to obtain some basic information on the spectrin–ankyrin interaction. The result would provide a reliable means to characterize the potential ability of the erythrocyte membrane skeleton to withstand externally applied mechanical stress. While dissociation constant is a legitimate candidate to describe the stability of a bond under equilibrium conditions, it is an indirect measure of the strength of a bond under applied force. A more direct measure would be obtained by the force spectroscopy method using an AFM or other force measuring apparatuses at the single molecular level [23–29]. Therefore, we adopted the force spectroscopy method based on the nano-mechanical capability of the AFM.

In this article, we report the result of measurement of the unbinding force of a non-covalently associating pair of spectrin and a recombinant ankyrin fragment, ankyrin 1. Ankyrin 1 was covalently immobilized on a cantilever and spectrin on the substrate, respectively. The two proteins were then gently brought into contact on the AFM sample stage by reducing the cantilever–substrate distance, then after a short time, the distance was gradually increased. When no binding was established between proteins on the cantilever and the substrate, the cantilever was not deflected. When the two proteins were bound to each other during a short contact time, the cantilever was increasingly deflected downward during its separation process from the substrate. This downward deflection of the cantilever was converted to force by multiplying the spring constant of the cantilever. As the force exerted to the interacting pair of the proteins reached and exceeded the threshold value of unbinding force, the cantilever was suddenly freed of the tensile load and jumped back to its un-deflected state. This jump in the force value was collected as the unbinding force of the associated pair of proteins. This technique has been widely used to measure the strength of non-covalently interacting macromolecular pairs [23–29]. As a closely related case to the present work, Afrin et al. have reported an unbinding analysis of delipidated erythrocyte cytoskeleton–Band 3 complex from concanavalin A on the AFM tip [12].

As a result, the unbinding force between spectrin and ankyrin 1 was found to be approximately 30 pN under a loading rate of 1.2 nN/s. The existence of two energy barriers in the process of unbinding was identified from the loading rate dependence of unbinding force. The parameters obtained from force spectroscopy experiments according to the Bell–Evans model [30,31], allow us to predict the acceleration of the unbinding rate of spectrin–ankyrin complex under an applied tensile force of arbitrary magnitude within a reasonably compatible range of loading rate with this experiment.

2. Materials and methods

2.1. Chemicals and proteins

Ni-NTA was purchased from Qiagen (Valencia, CA). Di-sodium phosphate, potassium phosphate, NaCl and imidazole were purchased from Wako Pure Chemical Industries (Osaka, Japan). Spectrin as an α- and β-complex from human erythrocyte, 3-aminopropyltriethoxysilane (APTES), N, N-diisopropylethylamine (DIPEA), 1,8-octanedithiol, 6-mercapto hexan-1-ol were purchased from Sigma-Aldrich (St. Louis, MO). N-hydroxy-succinimide-ester-polyethylene-glycol-maleimide (NHS-PEG-MAL) with the PEG part MW of 3400 Da was purchased from Nektar Therapeutics (San Carios, CA).

Goat polyclonal antibodies to spectrin βI (C-18) (sc-7466) which was used for immunoblotting and in AFM inhibition experiment, was obtained from (Santa Cruz Biotechnology, Santa Cruz, CA). Mouse monoclonal antibody to anti-*Strep* tag II which was used for immunoblotting was purchased from IBA (IBA, Gottingen, Germany).

2.2. Preparation of histidine conjugated spectrin binding domain of ankyrin 1

Total RNA was prepared from human erythroid using a FastPure RNA kit (TaKaRa Bio Inc., Shiga, Japan). cDNA was synthesized from the prepared RNA and the cDNA of spectrin binding domain of ankyrin 1 (called hereafter ANK1-62k) was amplified by PCR. His tag-ANK1-62k-*Strep* tag expression vector was constructed in the following way. The amplified DNA was digested with *Nde*I and *Sal*I, and then the digested DNA fragment was cloned into a modified pET15b vector which was digested again with *Nde*I and *Xho*I. The modified pET15b vector was inserted *Strep*-tag coding sequence following *BamH*I site. Although the amplified cDNA sequence had one SNP in its 631 nucleotides, the mature polypeptide had the same amino acid sequence as the published one.

The cloned vector was transformed into Rossetta 2 (DE3) competent *Escherichia coli* cells (Novagen, Madison, WI). The transformant was cultured up to the mid-log stage at 37 °C in Terrific broth supplemented with 100 μg/ml of ampicillin, then isopropyl-β-galactopyranoside (final concentration 1 mM) was added to induce ANK1-62k. It was cultured for another 3 h at 37 °C. The cells were then harvested and stored at −80 °C until use.

ANK1-62k was purified as described below. The cells were suspended in a phosphate buffered saline (PBS) supplemented with protease inhibitors (GE Healthcare, Little Chalfont, England) and disrupted completely by sonication. The resultant suspension was then centrifuged at 20,000 ×*g* at 4 °C for 20 min. The supernatant was collected and applied on a *Strep*-Tactin resin column (IBA, Gottingen, Germany) and passed through it. This process was repeated twice, then the resin was washed with the washing buffer to elute the bound protein. The first five milli-liter fractions of the eluted protein were pooled and ammonium sulfate was added to it at a final concentration of 500 mM. The pooled fraction was applied to a butyl-toyopearl 650 M column twice, then successively eluted with 50 mM Na-phosphate buffer (pH 7.0) containing 500 mM NaCl, each supplemented with 500 mM, 200 mM, 100 mM, 50 mM, 20 mM, and 10 mM of ammonium sulfate, respectively. The column was further eluted with the same buffer without supplementary ammonium sulfate. Fractions eluted with 200 and 100 mM ammonium sulfate were pooled as ANK1-62k after displacing the solvent with ammonium sulfate free buffer on an Amicon filter. The purity of the ANK1-62k sample prepared as above was confirmed to be better than 90% by SDS-PAGE and as satisfactory for our work.

2.3. Interaction analysis between spectrin and ANK1-62k

To obtain proof that the recombinant ANK1-62k had a specific affinity to commercially obtained spectrin, we performed an affinity chromatography before using it in AFM experiments.

The purified ANK1-62k and about 1 μg of spectrin were gently mixed with *Strep* Tactin resin beads for 2 h at 4 °C in 50 mM phosphate buffer (pH 7.5) containing 500 mM NaCl. After washing the beads with PBS five times, they were boiled in 1% SDS to detach bound proteins. The solubilized proteins were separated on SDS-PAGE and protein bands were transferred onto a polyvinylidene difluoride (PVDF) membrane (Pierce Biotechnology). After a blocking procedure with skim-milk, the membrane was probed with primary antibodies. After washing with PBS containing 0.1% Tween 20 (PBST) three times, the membranes were incubated with horseradish peroxidase-conjugated secondary antibodies. The membranes were then washed three times with PBST and the remaining signals were identified by a colorimetric method.

2.4. Preparation of mica substrate and AFM cantilever

Commercially available soft AFM cantilever probes, OMCL-TR400 PB-1 (both sides gold coated) with a nominal force constant of 0.09 nN/nm were provided by Olympus (Tokyo, Japan). The cantilever spring constants were determined by thermal noise analysis with the built-in software of the AFM system (MFP-3D, Asylum Research, Santa Barbara, CA) [32].

Cross-linking of ANK1-62k and spectrin to cantilever tips and mica substrates, respectively, was a three-step process as follows.

First, cantilevers and mica substrates were cleaned of organic contaminants in a UV ozone cleaner (NL-UV253, Nippon Laser and Electronics Lab., Tokyo, Japan). Cantilevers were incubated with 50 μl of 2 mM 1,8-octanedithiol and 50 μl of 20 mM 6-mercapto hexan-1-ol in ethanol for at least 18 h to introduce thiol-groups on the tip surface. The modified cantilevers were washed with ethanol and incubated for 20 min in 100 μl of ethanol containing 1 mg/ml of NHS-PEG-MAL in PBS. They were then washed several times with PBS to remove unreacted crosslinkers.

Freshly cleaved mica substrates were amino-silanized by exposing them to APTES vapor for 2 h in a 2-liter desiccator filled with argon gas and containing 30 μl APTES and 10 μl DIPEA in separate small vessels [33].

The amino-silanized mica substrates were incubated in a 1% glutaraldehyde for 60 min and then rinsed three times with MilliQ water to remove unreacted glutaraldehyde.

The glutaraldehyde modified pieces of mica as above were incubated in an aqueous solution of spectrin (0.2–1 mg/ml) for 60–120 min while the NHS-PEG-MAL modified cantilevers as above were incubated for 120 min in 0.5 mg/ml of ANK1-62k dissolved in PBS. Finally modified cantilevers and mica substrates were extensively washed with PBS containing 1% glycine to inactivate remaining reactive groups.

2.5. AFM force measurement

Force measurement experiments and imaging were performed on a commercial Asylum MFD-3D AFM (Asylum Research). AFM images of crosslinked spectrin molecules to a mica surface were collected in PBS at room temperature in AC mode. The images were captured in a scan size of 2.5 × 2.5 μm and with a resolution of 256 × 256 pixels. The height image was linearly plane-fitted and flattened. In the force map mode of the AFM, the tip alternately approached to and retracted from 24 × 24 points over a 2.5 × 2.5 μm sample surface while force curves were synchronously recorded at room temperature in PBS. The dwell time between the cantilever and the substrate was set to 0.08 s, long enough to form spectrin–ankyrin complex but short enough to reduce the frequency of the non-specific interaction. A dynamic force spectroscopy study was achieved by varying the retraction speed of cantilever from 32 nm/s to 2500 nm/s and retraction distance between 50 nm and 5000 nm.

2.6. Data analysis

Force curves were analyzed using a home developed software on IGOR pro (WaveMetrics, Lake Oswego, OR). The most probable

unbinding force in each set of experiment was obtained from the histogram of approximately 500 raw data. Histograms were fitted with a Gaussian fitting curve multiplied by a window function to account for the limiting force sensitivity. The apparent loading rate was defined as the slope of the force curve just before the final rupture event. Errors in the determination of the mean of the distribution and in the cantilever spring constant uncertainty were taken into account as the uncertainties in mean unbinding force and loading rate determination. Mean unbinding lengths were obtained similarly while the uncertainty was given by the standard error of the mean. Detailed description of these methods can be found in our previous publication [25,34].

3. Results

3.1. Confirmation of binding of ANK1-62k to spectrin by affinity chromatography method

To confirm that the recombinant ANK1-62k had a binding activity to commercially obtained α-, β-spectrin complex (to be called spectrin hereafter), we performed an affinity chromatography experiment as follows.

The purity of recombinant ANK1-62k and commercially obtained spectrin was confirmed by SDS-PAGE to be satisfactory for our purpose as shown in Fig. 1A. The major band at about 60 kDa corresponded to purified ANK1-62k while a few minor bands around 50 kDa were contaminants. The purity of ANK1-62k was estimated to be 90% or better. In the case of spectrin, we detected major signals around 250 kDa which corresponded to α- and β-spectrin. Additionally a minor band at about 45 kDa was detected as a contaminant.

Next we assayed the interaction between purified ANK1-62k and β-spectrin *in vitro* using affinity column chromatography as described in Materials and methods. The C-terminal of recombinant ANK1-62k was fused with the *Strep* tag II which has a specific interaction with *Strep* Tactin resin, so that the presence of ANK1-62k was detected at about 60 kDa using anti-*Strep* tag II antibodies. Using this affinity, we carried out a pull down assay to detect the ANK1-62k and β-spectrin complex as described above. The result shown in Fig. 1B indicated that although spectrin had non-zero affinity to the resin beads in the absence of ANK1-62k, its binding to the beads was significantly enhanced in the presence of ANK1-62k. The result confirmed that the purified ANK1-62k had binding activity to spectrin.

3.2. Most probable unbinding force between ANK1-62k and spectrin

To investigate the interactions between ANK1-62k and β-spectrin at the single-molecule level, we used the AFM to acquire force mapping data. ANK1-62k molecules were cross-linked to the tip via a heterobifunctional PEG cross-linker and spectrin was similarly cross-linked to a flat mica substrate as schematized in Fig. 2.

The image in Fig. 3A was captured with a modified AFM tip with ANK1-62k so that force curve measurement could be performed in the same area without changing the cantilever. Many fibrous molecules

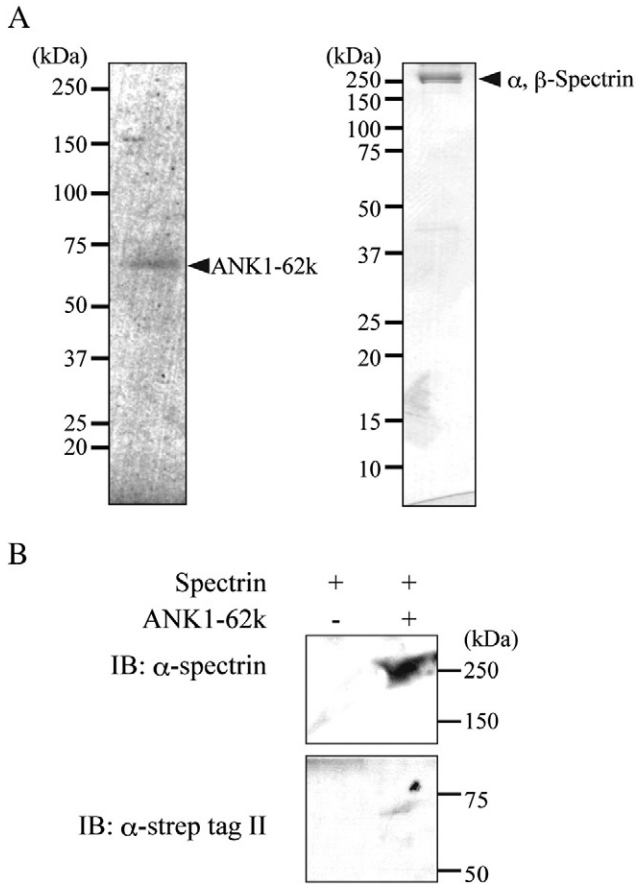

Fig. 1. Interaction analysis between recombinant ANKI-62k and spectrin *in vitro*. (A) SDS-PAGE patterns of purified recombinant ANKI-62k and commercially obtained spectrin. Gels were stained with CBB. (B) Spectrin was incubated with *Strep*-Tactin resin in the presence or absence of recombinant ANKI-62k. After SDS-PAGE of the proteins bound to the resin, they were probed by immunoblotting with anti-spectrin and anti-*Strep* tag II antibodies.

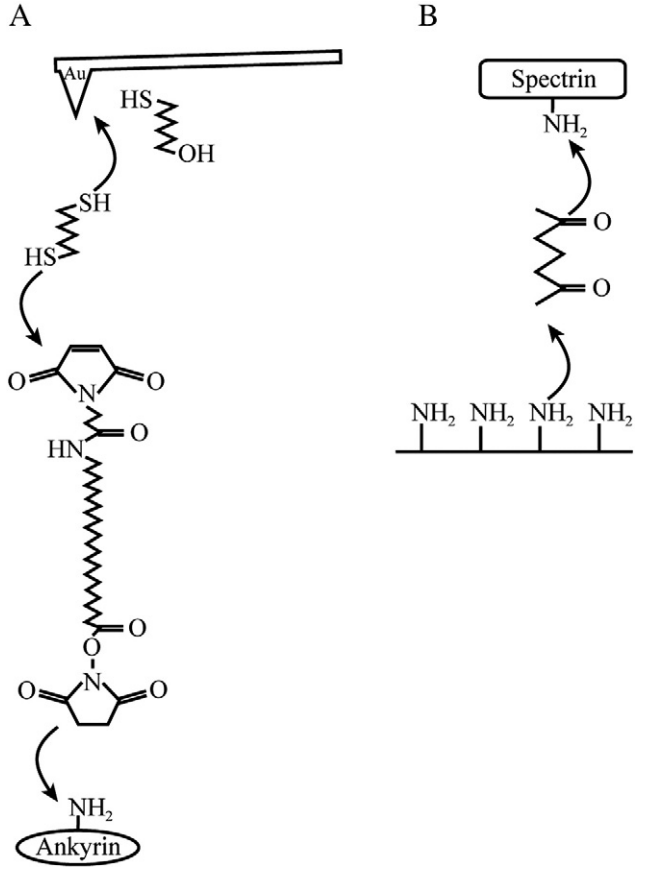

Fig. 2. Three-step cross-linking of AFM tip and samples. (A) 1. Gold-coated tips were modified by incubation with 1,8-octanedithiol and 6-mercapto-hexan-l-ol. 2. Heterobifunctional PEG linker was anchored to the thiol bearing tips through the maleimide end. 3. Recombinant ANK1-62k was finally cross-linked to the tip via reaction to the NHS end of PEG. (B) 1. Mica was amino-silanized by exposure to APTES vapor. 2. Glutaraldehyde was attached to amino-groups on amino-silanized mica through one of its aldehyde ends. 3. Spectrin was cross-linked to the aldehyde on mica.

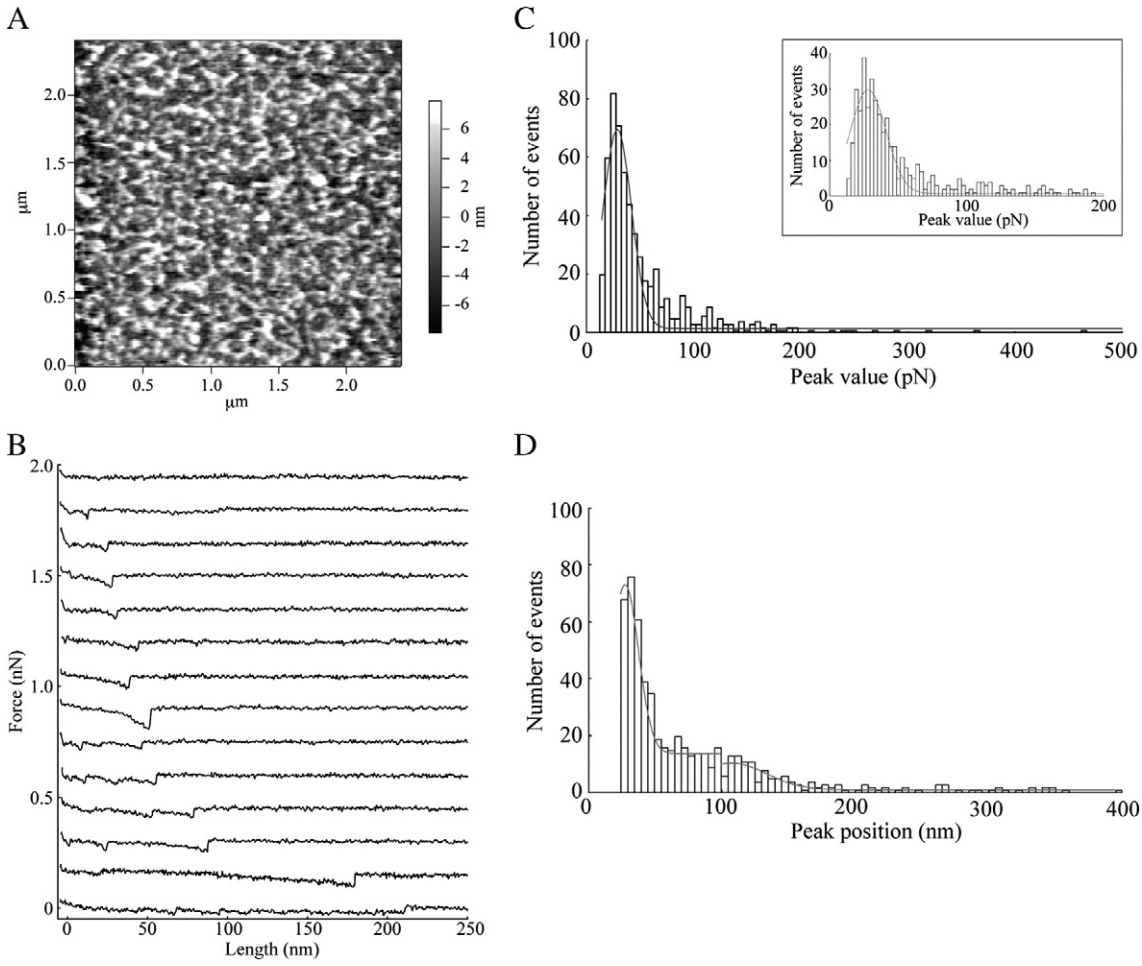

Fig. 3. Force spectroscopy results between purified recombinant ANK1-62k and spectrin. (A) AFM height image of immobilized spectrin on mica in PBS. Resolution is 256 × 256 pixels in 2.5 μm × 2.5 μm scan area. (B) Retraction force curves obtained in PBS with spectrin on mica and ANK1-62k on AFM tip. The ordinate represents cantilever force (=deflection × force constant) and the abscissa the cantilever retraction distance here and in the following force curve diagrams. (C) Histogram of 571 unbinding force values obtained after analysis of 4028 force curves. The mean unbinding force value was 28.62 ± 0.55 pN (mean ± SEM, here and hereafter). The insert shows force histogram in the peak position ranges from 0 to 100 nm and the mean unbinding force value was 28.05 ± 0.62 pN. (D) Unbinding length distribution for the events plotted in B, showing two peak at unbinding lengths of 27.07 ± 0.49 and 107.06 ± 2.21 nm.

were identified in the image with an approximate length and width of 200–300 nm (or longer) 20–30 nm, respectively. Those in 200–300 nm range in length were considered as spectrin tetramer, whereas, longer one as either overlapped or aggregated spectrins.

AFM force curves were then recorded in PBS at pH 7.4. The spring constant of the cantilever used in this experiment was 0.089 nN/nm as found by thermal tuning method. The approach tip velocity was ~800 nm/s. Force curves were analyzed as described above. In a typical force curve, a gradually but non-linearly increasing downward deflection starting from the zero deflection level was abruptly terminated with a jump to the zero force level. The initial low force deflection was due to an extension of the PEG part of the crosslinker taking place before ANK1-62k was separated from β-spectrin. In contrast, force curves having almost a linear increase of downward deflection with little separation from the substrate surface were considered to be due to non-specific adhesion events and excluded from our analysis. A small number of force curves had tandemly repeating force peaks that could be due to unfolding of spectrin domains. Since our interest was in the analysis of protein–protein interaction rather than protein unfolding, we collected only the last force peak as corresponding to unbinding of the two proteins.

A total of 4028 force curves were recorded over different spots on the substrate and several hundreds of them satisfying the above criteria for specific unbinding events were collected (571 events, i.e., ~14% to the total). The collected force curves were then analyzed and plotted in the form of histograms with respect to the mean unbinding force and extension length in Fig. 3.

A clear single peak arose in the histogram of force distribution and yielded a mean unbinding force of 28.62 ± 0.55 pN (mean ± SEM), where SEM is for standard error of the mean (the same hereinafter). The distribution of unbinding length (cantilever tip-sample distance at unbinding time) for these events showed a clear peak centered at 27.07 ± 0.49 nm corresponding nicely to the length of PEG linker (Fig. 3). These values did not change when the proteins on the tip and the substrate were exchanged. Since spectrin molecules were covalently immobilized on the substrate, it was highly unlikely that they were detached from the substrate with less than 1 nN force. It is, however, still possible that segments of loosely adsorbed spectrin molecules were lifted up trailing behind ANK-62k. It is very likely that the force curves extending to 100 nm range before the final rupture were due to such lift-up events.

To verify the specificity of the binding/unbinding events measured here, we performed further experiments in the presence of an inhibitor of binding, i.e., anti-spectrin antibody that binds to β-spectrin at a site close to ankyrin binding site. After recording force curves in the absence of the antibody, the same mica substrate loaded with spectrin was incubated in a solution containing 2 μg/ml anti-spectrin antibodies for 30 min. It was then washed three times with PBST. About 5800 new

force curves were recorded with the same cantilever. As shown in Fig. 4, the number of specific unbinding events decreased to ~42% of what was observed before antibody treatment. If we count only those events occurring with less than 100 nm extension, the probability fell to ~25%. The mean unbinding force obtained from force curves with longer extension than 100 nm was 19.68 ± 0.72 pN, significantly less than what was obtained in the absence of the antibody (Fig. 4). The mean unbinding force obtained from force curves having an extension of less than 100 nm was 25.90 ± 0.96 pN (127 events of a total 5758 curves, i.e., 2.2%). This value was similar when compared with those obtained in the absence of antibody in the same range of extension, i.e., 28.05 ± 0.62 pN (432 events of a total 4028 curves, i.e., ~10%). A possible reason that the inhibition was not complete was that antibodies might have been dissociated from β-spectrin during washing and force measurement procedures allowing the exposed binding sites on β-spectrins to react with ANK1-62k on the substrate.

3.3. Dynamic force spectroscopy of ANK1-62k–β spectrin complexes

To investigate the unbinding kinetics of the ANK1-62k β-spectrin complex, we recorded and analyzed minimum of 2000 force curves recorded under various tip retraction speeds (consequently different loading rates). The spring constant of the cantilevers used in this experiment was 0.093–0.105 nN/nm as found by thermal tuning method. Histograms of mean unbinding force at different loading rates are given in Fig. S2. While the measured loading rate ranged from 0.14 nN/s to 13.75 nN/s, the corresponding mean unbinding force varied from 20.95 pN to 48.13 pN.

We then plotted the mean unbinding force as a function of the logarithm of the loading rate in Fig. 5A and adapted the result to a commonly used Bell–Evans model. The model describes a transition from bound to unbound state as a separating process of a bond from a potential well across one or more activation energy barriers [29,30]. When a constant external force, f, is applied to the interaction between ANK1-62k and β spectrin, the dissociation process is facilitated due to lowering of the energy barriers resulting in an increased dissociation rate constant $k_{off}(f)$ as [35]:

$$k_{off}(f) = k_{off} exp(f\Delta x/k_B T) \quad (1)$$

where k_{off} is the intrinsic dissociation rate (i.e., the dissociation rate constant under zero external force), Δx is the distance between the maximum and minimum of the interaction potential along the direction of applied force, k_B is the Boltzmann constant and T is temperature in Kelvin. When the applied force increases with a loading rate r_f, the most probable unbinding force, f^*, can be written as:

$$f^* = (k_B T/\Delta x) ln(\Delta x/k_{off} k_B T) + (k_B T/\Delta x) ln\left(r_f\right). \quad (2)$$

The semi-logarithmic plot in Fig. 5 shows that the mean unbinding force depends linearly on ln (loading rate) with two different slopes in lower and higher loading rate regimes under our experimental conditions. The inflection point of the graph was at ~3.54 nN/s. By fitting experimental data to Eq. (2), parameters concerning interaction between ANK1-62 k and β-spectrin were obtained as $\Delta x = 1.73$ nm and $k_{off} = 0.0101\ s^{-1}$ between 0.14 to 3.54 nN/s and $\Delta x = 0.23$ nm and $k_{off} = 52.0\ s^{-1}$ above 3.54 nN/s. Our measurements provided an energy diagram of unbinding pathway that involved two energy barriers.

Previous analysis of surface plasmon resonance indicated that the dissociation constant K_D of ankyrin 1 (ZU5)–spectrin was 15.2 nM and the dissociation rate constant $k_{off} = 5.45 \times 10^{-2}\ s^{-1}$ [36]. Our result is in reasonable agreement with the k_{off} value cited above.

An approximate geometry of the energy landscape for the interaction between ANK1-62k and β-spectrin is presented in Fig. 5B with two activation barriers at a positions 0.23 nm and 1.73 nm, respectively, from the equilibrium distance.

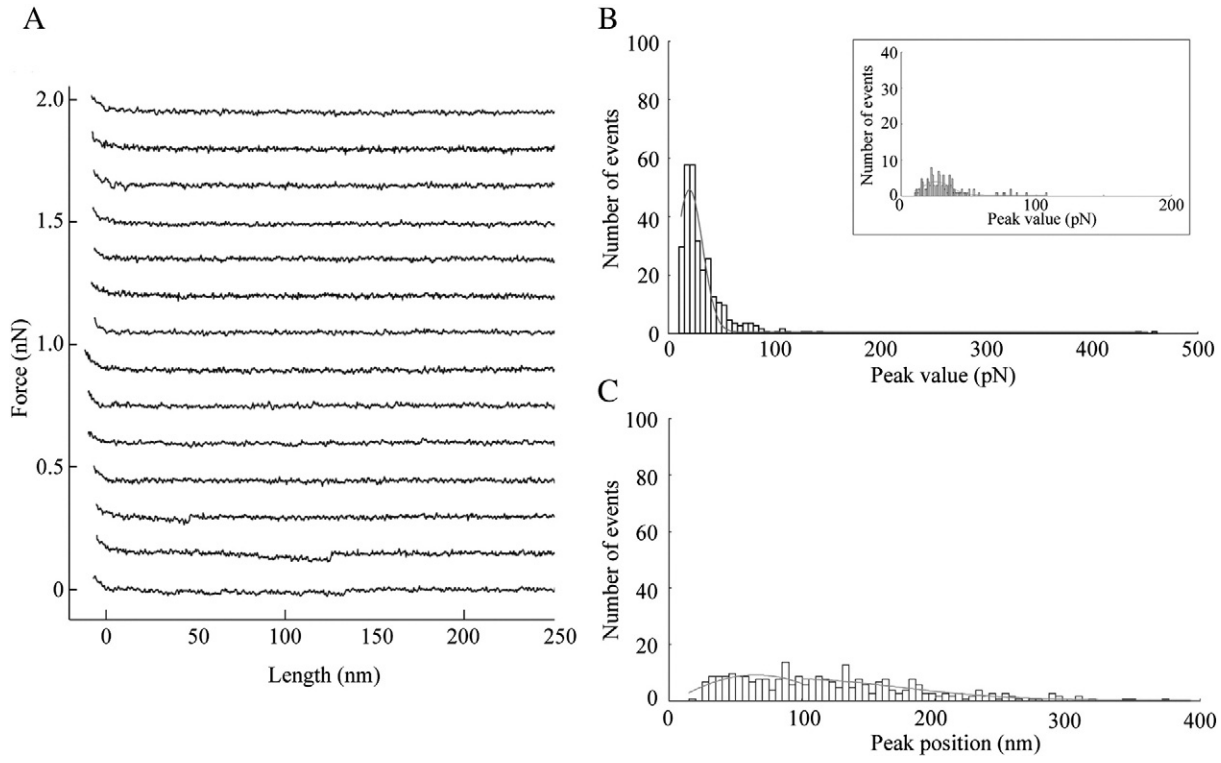

Fig. 4. Inhibition of ANKl-62k and spectrin interaction after treatment of spectrin with anti-spectrin polyclonal antibody. (A) The retraction force curves obtained in PBS. (B) Force histogram of 295 peak force obtained after analysis of 5758 force curves. The mean unbinding force value was 19.68 ± 0.72 pN. The insert shows force histogram of the peak position ranging from 0 to 100 nm and the mean unbinding force value was 25.90 ± 0.96 pN. (C) Unbinding length distribution for the events plotted in B, showing two peak at unbinding lengths of 65.32 ± 9.18 and 89.81 ± 6.46 nm.

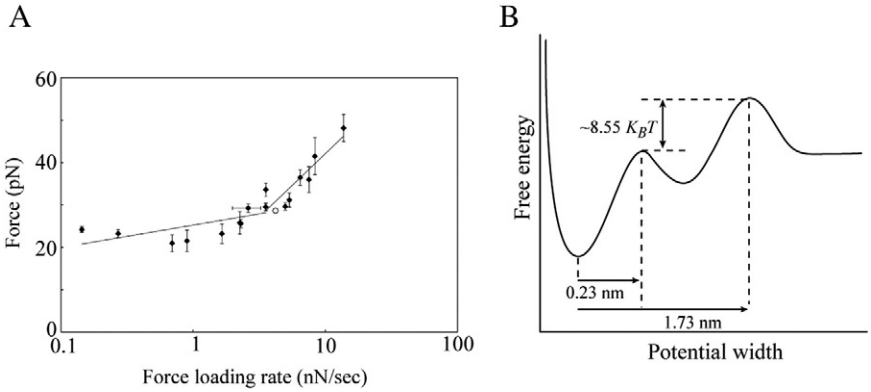

Fig. 5. Loading rate dependence of peak force. (A) The most probable unbinding force was plotted as a function of the logarithm of loading rate. The solid lines represent the result of linear fitting lines with different slopes. The open circle represents the unbinding force as shown Fig. 3. (B) Energy landscape of the complex between ANKl-62k and spectrin. The dissociation of ANKl-62k–β-spectrin complex involves overcoming two activation barriers.

4. Discussion

We studied *in vitro* unbinding mechanics of ANK1-62k–β-spectrin complex using the single molecule spectroscopy capability of the AFM as a model of ankyrin–β-spectrin interaction in the RBC membrane skeleton. This particular protein pair constitutes the most numerous, therefore, the major linking paths that secure seamless association of spectrin-based cytoskeleton and the phospholipid-based plasma membrane in the RBC membrane skeleton. ANK1-62k, a recombinant fragment of ankyrin, has an intact spectrin binding sequence and its binding activity was confirmed by a blotting experiment. As a result, about 30% of the force curves obtained in our AFM force spectroscopy experiment showed positive features of transient complex formation between the two proteins. From such force curves, we obtained the unbinding force of the pair under an externally applied tensile force.

We focused on the ankyrin–β-spectrin interaction because it is at the front end of the linking system in focus and yet thermodynamically less stable compared with Band 3–ankyrin association [11,36]. It is legitimate to ask how strong is the seemingly labile link in a chain of protein association between plasma membrane and the spectrin based cytoskeleton. It has been proposed that rapid dissociation and re-association of some parts of protein links is taking place during large scale deformation of RBC [22,37]. It is, therefore, especially important to compare the force to induce RBC shape change and the unbinding force of the weakest link.

It has been shown in our previous work that the delipidated RBC cytoskeleton could be pulled up to a few μm with an application of up to 70 pN of tensile force under a similar loading rate as above [12]. It is, therefore, not necessary to assume unbinding of spectrin network from the plasma membrane during a local deformation of an RBC even under a strongly localized tensile force. In the case of global deformation, the external force should be broadly dispersed over the entire cytoskeleton and the tensile force exerted on individual linkage sites would be much smaller than the case of localized force discussed above. Anong et al. reported the dissociation rate constant between Band 3 and ankyrin to be 0.060 min^{-1} (0.001 s^{-1}) [36] which is almost the same as our dissociation rate constant for ankyrin–β-spectrin pair at the lower loading rate regime. We think that Band 3 survives detergent treatment of RBC only when it is bound to spectrin via ankyrin. Our result suggests that, if there is a case of dissociation of a part of the spectrin network from the lipid membrane, ankyrin–β-spectrin bond would be broken faster than the one between ankyrin–Band 3. Therefore, this bond would become the weakest link.

Dao et al. [38] reported that a global deformation of RBC can be induced with a force less than ~300 pN when the cell was pulled to opposite directions using two beads (diameter = 4.12 μm) attached diametrically opposite points as force transducers. From the size of the bead and the average density of Band 3–ankyrin–spectrin linkage system, the force loaded on a single linkage would be very small. Even under a tensile force of such small magnitude, it would still be possible that spectrin unfolding takes place in competition with the rupture of ankyrin–β-spectrin bond if the duration of force application was long. The unfolding force [14] is, indeed, similar to our unbinding force.

The energetic diagram of ankyrin 1–β-spectrin association reaction was obtained showing two energy barriers within the available loading rate range in our experiment. The data indicated that the ANK1-62 k–β-spectrin complex overcomes two free energy barriers during unbinding. The difference in activation free energy between the inner and the outer barriers, $\Delta G^{\ddagger} = -k_B T \ln(k^1_{off} / k^2_{off})$, where k^1_{off} and k^2_{off} are the Bell model parameters k_{off} for the inner and outer barrier, respectively, turned out to be in the range of ~8.55 k_BT.

Our results and those in previous papers indicated that the unbinding force of ankyrin from spectrin is almost one half of the unbinding force of Band 3 from spectrin. Interestingly, in this context, Ipsaro and Mondragon have shown that one ankyrin binds to one β-spectrin molecule [39]. Kim et al. [40] have, further, shown that two Band 3 molecules are bound to one ankyrin molecule. These results indicate that Band 3–anykrin–spectrin interaction has 2:1:1 stoichiometry. Each spectrin tetramer, which involves two β-spectrin molecules, interacts with two ankyrin molecules and consequently binds four Band 3 molecules. Therefore our data would complement the proposed cooperativity between ankyrins in binding to β-spectrin [41].

A model of RBC deformation involving not only bending and stretching of the membrane skeleton but also un-binding and re-binding of non-covalently associated protein pairs has been proposed to accommodate a large scale and rapid shape changes [21,37]. It has been reported that helix C of spectrin repeat H14 is slightly pulled to ZU5 domain of ankyrin in spectrin–ankyrin complex and loop B/C of spectrin repeat H15 interacts with ZU5 domain of ankyrin [39,42]. These conformational changes might cause a mild degree of compression and/or extension of spectrin bound to ankyrin and help unfold spectrin repeat. We think that unbinding event of β-spectrin–ankyrin pair during even most drastic deformation of RBC is a rare event, if at all, under physiologically relevant mechanical conditions. Girasole et al. reported that the roughness of red blood cells was hardly changed after drying and staining treatment keeping the membrane–cytoskeleton functional [43]. They also suggested that the membrane–cytoskeleton linkage was weakened by lipid oxidation that was due to reduction of intracellular ATP concentration in aging RBC. Since the linkage of the membrane–cytoskeleton may become weakened, the ankyrin–spectrin interaction also is possibly weakened in aging of RBC.

The biological relevance of the measured unbinding force should be understood from the perspective of force balance in the membrane skeleton network. Under physiological conditions in the blood vessels, RBC

is under a shear stress of 10–100 Pa, which, when interpreted as a force on individual ankyrin–β-spectrin pair, could be estimated as in the range of a few pico-newtons. Thus the measured tensile strength of the pairwise interaction bond would be strong enough to withstand the external stress. The non-covalent associations in the network have survived the test of evolution if it is at best strong enough to keep the functional conformation of RBC during its lifetime.

Supplementary data to this article can be found online at http://dx.doi.org/10.1016/j.bpc.2015.03.007.

Acknowledgments

This work was supported by Grants-in-Aid for Creative Scientific Research (19GS0418) to A. I. from the Japan Society for the Promotion of Science (JSPS).

References

[1] D. Boal, Mechanics of the Cell, Cambridge Univ. Press, Cambridge, 2002.
[2] D.E. Discher, New insights into erythrocyte membrane organization and microelasticity, Curr. Opin. Hematol. 7 (2000) 117–122.
[3] E.A. Evans, Structure and deformation properties of red blood cells: concepts and quantitative methods, Methods Enzymol. 173 (1989) 3–35.
[4] V. Bennett, The molecular basis for membrane–cytoskeleton association in human erythrocytes, J. Cell. Biochem. 18 (1982) 49–65.
[5] T.J. Byers, D. Branton, Visualization of the protein associations in the erythrocyte membrane skeleton, Proc. Natl. Acad. Sci. U. S. A. 82 (1985) 6153–6157.
[6] P. Agre, J. Parker, Red Blood Cell Membranes: Structure, Function Clinical Implications, Marcel Dekker, New York., 1989
[7] N.S. Gov, S.A. Safran, Red blood cell membrane fluctuations and shape controlled by ATP-induced cytoskeletal defects, Biophys. J. 88 (2005) 1859–1874.
[8] D.T. Mirijanian, G.A. Voth, Unique elastic properties of the spectrin tetramer as revealed by multiscale coarse-grained modeling, Proc. Natl. Acad. Sci. U. S. A. 105 (2008) 1204–1208.
[9] J. Palek, S.C. Liu, Red cell membrane skeleton: structure–function relationships, Prog. Clin. Biol. Res. 43 (1980) 21–44.
[10] A.J. Baines, Evolution of spectrin function in cytoskeletal and membrane networks, Biochem. Soc. Trans. 37 (2009) 796–803.
[11] J.J. Ipsaro, L. Huang, L. Gutierrez, R.I. MacDonald, Molecular epitopes of the ankyrin–spectrin interaction, Biochemistry 47 (2008) 7452–7464.
[12] R. Afrin, M. Nakaji, H. Sekiguchi, D. Lee, K. Kishimoto, A. Ikai, Forced extension of delipidated red blood cell cytoskeleton with little indication of spectrin unfolding, Cytoskeleton 69 (2012) 101–112.
[13] D.E. Discher, P. Carl, New insights into red cell network structure, elasticity, and spectrin unfolding—a current review, Cell. Mol. Biol. Lett. 6 (2001) 593–606.
[14] M. Rief, J. Pascual, M. Saraste, H.E. Gaub, Single molecule force spectroscopy of spectrin repeats: low unfolding forces in helix bundles, J. Mol. Biol. 286 (1999) 553–561.
[15] W. Lee, X. Zeng, K. Rotolo, M. Yang, C.J. Schofield, V. Bennett, W. Yang, P.E. Marszalek, Mechanical anisotropy of ankyrin repeats, Biophys. J. 102 (2012) 1118–1126.
[16] J.C. Pinder, K.S. Smith, A. Pekrun, W.B. Gratzer, Preparation and properties of human red-cell ankyrin, Biochem. J. 264 (1989) 423–428.
[17] A. Nans, N. Mohandas, D.L. Stokes, Native ultrastructure of the red cell cytoskeleton by cryo-electron tomography, Biophys. J. 101 (2011) 2341–2350.
[18] Y. Ohta, H. Okamoto, M. Kanno, T. Okuda, Atomic force microscopic observation of mechanically traumatized erythrocytes, Artif. Organs 26 (2002) 10–17.
[19] T. Mizuno, T. Tsukiya, Y. Taenaka, E. Tatsumi, T. Nishinaka, H. Ohnishi, M. Oshikawa, K. Sato, K. Shioya, Y. Takewa, H. Takano, Ultrastructural alterations in red blood cell membranes exposed to shear stress, ASAIO J. 48 (2002) 668–670.
[20] C.P. Johnson, H.Y. Tang, C. Carag, D.W. Speicher, D.E. Discher, Forced unfolding of proteins within cells, Science 317 (2007) 663–666.
[21] C.C. Krieger, X. An, H.Y. Tang, N. Mohandas, D.W. Speicher, D.E. Discher, Cysteine shotgun-mass spectrometry (CS-MS) reveals dynamic sequence of protein structure changes within mutant and stressed cells, Proc. Natl. Acad. Sci. U. S. A. 108 (2011) 8269–8274.
[22] X. An, M.C. Lecomte, J.A. Chasis, N. Mohandas, W. Gratzer, Shear-response of the spectrin dimer–tetramer equilibrium in the red blood cell membrane, J. Biol. Chem. 277 (2002) 31796–31800.
[23] E.L. Florin, V.T. Moy, H.E. Gaub, Adhesion forces between individual ligand–receptor pairs, Science 264 (1994) 415–417.
[24] V.T. Moy, E.L. Florin, H.E. Gaub, Intermolecular forces and energies between ligands and receptors, Science 266 (1994) 257–259.
[25] A. Yersin, T. Osada, A. Ikai, Exploring transferrin–receptor interactions at the single-molecule level, Biophys. J. 94 (2008) 230–240.
[26] P. Hinterdorfer, Y.F. Dufrene, Detection and localization of single molecular recognition events using atomic force microscopy, Nat. Methods 3 (2006) 347–355.
[27] M. Gad, A. Itoh, A. Ikai, Mapping cell wall polysaccharides of living microbial cells using atomic force microscopy, Cell Biol. Int. 21 (1997) 697–706.
[28] P.P. Lehenkari, M.A. Horton, Single integrin molecule adhesion forces in intact cells measured by atomic force microscopy, Biochem. Biophys. Res. Commun. 259 (1999) 645–650.
[29] C. Yuan, A. Chen, P. Kolb, V.T. Moy, Energy landscape of streptavidin–biotin complexes measured by atomic force microscopy, Biochemistry 39 (2000) 10219–10223.
[30] E. Evans, Energy landscapes of biomolecular adhesion and receptor anchoring at interfaces explored with dynamic force spectroscopy, Faraday Discuss. 111 (1998) 1–16.
[31] E. Evans, Looking inside molecular bonds at biological interfaces with dynamic force spectroscopy, Biophys. Chem. 82 (1999) 83–97.
[32] J.L. Hutter, J. Bechhoefer, Calibration of atomic-force microscope tips, Rev. Sci. Instrum. 64 (1993) 1868–1873.
[33] C. Stroh, H. Wang, R. Bash, B. Ashcroft, J. Nelson, H. Gruber, D. Lohr, S.M. Lindsay, P. Hinterdorfer, Single-molecule recognition imaging microscopy, Proc. Natl. Acad. Sci. U. S. A. 101 (2004) 12503–12507.
[34] C. Yan, A. Yersin, R. Afrin, H. Sekiguchi, A. Ikai, Single molecular dynamic interactions between glycophorin A and lectin as probed by atomic force microscopy, Biophys. Chem. 144 (2009) 72–77.
[35] E. Evans, K. Ritchie, Dynamic strength of molecular adhesion bonds, Biophys. J. 72 (1997) 1541–1555.
[36] W.A. Anong, T.L. Weis, P.S. Low, Rate of rupture and reattachment of the band 3–ankyrin bridge on the human erythrocyte membrane, J. Biol. Chem. 281 (2006) 22360–22366.
[37] Z. Peng, R.J. Asaro, Q. Zhu, Multiscale simulation of erythrocyte membranes, Phys. Rev. E Stat. Nonlinear Soft Matter Phys. 81 (2010) 031904.
[38] M. Dao, C.T. Lim, S. Suresh, Mechanics of the human red blood cell deformed by optical tweezers, J. Mech. Phys. Solids 51 (2003) 2259–2280.
[39] J.J. Ipsaro, A. Mondragon, Structural basis for spectrin recognition by ankyrin, Blood 115 (2010) 4093–4101.
[40] S. Kim, S. Brandon, Z. Zhou, C.E. Cobb, S.J. Edwards, C.W. Moth, C.S. Parry, J.A. Smith, T.P. Lybrand, E.J. Hustedt, A.H. Beth, Determination of structural models of the complex between the cytoplasmic domain of erythrocyte band 3 and ankyrin-R repeats 13–24, J. Biol. Chem. 286 (2011) 20746–20757.
[41] C.D. Cianci, M. Giorgi, J.S. Morrow, Phosphorylation of ankyrin down-regulates its cooperative interaction with spectrin and protein 3, J. Cell. Biochem. 37 (1988) 301–315.
[42] P.R. Stabach, I. Simonovic, M.A. Ranieri, M.S. Aboodi, T.A. Steitz, M. Somonovic, J.S. Morrow, The structure of the ankyrin-binding site of β-spectrin reveals how tandem spectrin-repeats generate unique ligand-binding properties, Blood 113 (2009) 5377–5384.
[43] M. Girasole, S. Dinarelli, G. Boumis, Structure and funciton in native and pathological erythrocytes: a quantitative view from the nanoscale, Micron 43 (2012) 1273–1286.